Bifocal Reflector Antenna System for Radar Imaging at 300 GHz

Antonio García-Pino[1], Borja Gonzalez-Valdes[1], Beatriz Mencia-Oliva[2], Jesús Grajal de la Fuente[2], Oscar Rubiños López[1], and José Luis Besada Sanmartín[2]

[1] Dpto. De Teoría do Sinal e Comunicacións, Universidade de Vigo. Rúa Maxwell s/n, Campus Universitario, 36310 Vigo, Spain. Email: {agpino, bgvaldes, oscar}@com.uvigo.es

[2] Dpto. de Señales, Sistemas y Radiocomunicaciones, ETSI Telecomunicación. Universidad Politécnica de Madrid, Ciudad Universitaria s/n 28040 Madrid, Spain. Email: {bmencia,jesus}@gmr.ssr.upm.es; besada@gr.ssr.upm.es

***Abstract*—A 300 GHz radar imaging system is presented, including descriptions of the radar sensor and antenna subsystems. The antenna consists of a Bifocal Ellipsoidal Gregorian Reflector whose beam is scanned by a combination of the rotation and vertical tilting of a flat small secondary mirror. A prototype is being mounted and its characterization will be presented.**

Index Terms— Reflector antennas, scanning antennas, submillimeter-wavelength imaging

I. INTRODUCTION

The detection of weapons or contraband concealed on persons have been solved by methods that require the sensor and the target to be in close proximity, such as trace chemical sniffers or X-ray imaging systems. For situations that call for standoff observation, concealed weapons detection is extremely difficult to accomplish. Active sub-millimeter-wave imaging has demonstrated to be a promising technique to achieve through-clothing imaging at standoff ranges from 5 to 100 m. Between 100 GHz and 1 THz, high image resolution of about 1cm can be achieved with a compact aperture. Besides, a wide range of materials (clothing, paper, plastic, wood ...) is reasonably transmissive [1,2] in this band.

Due to the technological difficulty of having focal plane arrays at these frequencies, mechanical fast beam scanning has been proposed to interrogate the interest area in a pixel by pixel imaging configuration. This communication presents the description of the imaging system, including the details of the antenna and radar subsystems

II. RADAR SENSOR AT 300 GHZ

This section presents a continuous-wave linear-frequency modulation (CW-LFM) high-resolution radar sensor. The operational bandwidth goes from 286.2 to 313.2 GHz, within a window of atmospheric attenuation. Sub-cm range resolution is attained by the use of 27-GHz bandwidth. This homodyne prototype is composed of commercial-off-the-shelf (COTS) components and designed-specific circuits. This system is the upgrade of a previously reported radar sensor working at 100 GHz [3,4]. Its architecture, based on frequency-multiplying and amplification stages, makes the system easily scalable to higher frequencies. The radar structure can be divided into three different parts, corresponding to the technologies involved in the design (Fig. 1).

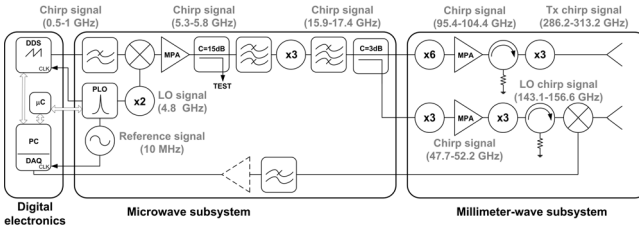

Figure 1. Block diagram of the 300-GHz radar sensor

The digital electronics subsystem includes the chirp signal generation by means of a DDS module, which ensures the linearity of the transmitted chirp waveform, a digitizer for data acquisition, a microcontroller in charge of the initial configuration and a conventional PC. The microwave subsystem is based on encapsulated MMICs and other commercial surface-mount technology (SMT) components, assembled on custom-made microstrip technology circuits. The chirp signal ramps over 1.5 GHz, from 15.9 to 17.4 GHz.

Finally, the millimeter-wave subsystem includes both transmitter and receiver (Fig. 1). The former is based on a ×6 frequency multiplier-amplifier - isolator - ×3 frequency multiplier chain. The latter is based on a subharmonic mixer, which is in charge of the demodulation of the received signal.

The LO input signal (143.1-156.6 GHz) is obtained by means of frequency multiplication from the output signal of the microwave subsystem. The chirp signal at 286.2-313.2 GHz with 0-dBm power level is transmitted through a silicon beamsplitter, acting as a circulator to isolate transmitter and receiver, towards the antenna subsystem. The reflected signal reaches the subharmonic mixer to be demodulated. It should be pointed out that this subsystem is based on components implemented in waveguide technology since it is beneficial in terms of power handling and shock and corrosion resistance.

Fig. 2 shows (a) the signal generation module as part of the digital electronics subsystem and the microwave modules, and (b) the transmitter and receiver chains, corresponding to the millimeter-wave subsystem.

978-88-907018-1-8/13/$31.00 ©2013 IEEE

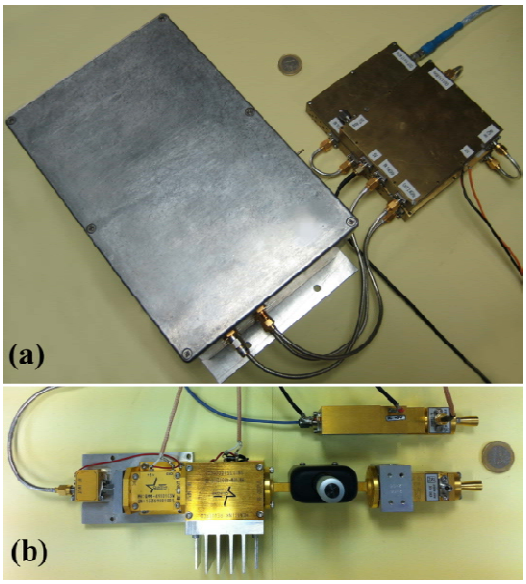

Figure 2. Radar sensor: (a) signal generation and microwave modules; (b) millimeter-wave subsystem: transmitter (top) and receiver (bottom) chains.

III. REFLECTOR ANTENNNA SYSTEM

A. General description of the antenna configuration

The radiating subsystem (tx/rx) has critical impact on the design of the radar to meet the aforementioned objective (high image resolution and fast image acquisition with a compact aperture at a standoff range of 8 m at 300 GHz). Due to the technological difficulty of fabricating focal plane arrays at this band, a multi-reflector antenna (Fig.3) based on the rotation of a small, flat and lightweight mirror has been proposed [5-6]:

(a-b) The **main reflector and the subreflector** are shaped surfaces configured as the Bifocal Ellipsoidal Gregorian Reflector System (BEGRS) described in [6], in order to improve the scanning behavior of the antenna, provide higher field of view, increase the antenna gain in the target region and allow better control of the scanning operation. In addition, the subreflector must be oversized in order to span the field of view to the size of the human torso.

(c) In order to provide scanning characteristics, the illuminating wave arrives at the subreflector after being reflected in the aforementioned **mirror**. The fast rotation of this mirror and the slow tilting of its rotation axis allow the fast scanning operation of the antenna.

(d) A **feed reflector** designed to illuminate the subreflector with a tapered collimated beam.

(e) A **silicon beamsplitter** to separate the transmitted and received beams.

B. BEGRS shaped design

The baseline configuration of the main reflector and subreflector is shown in Fig. 4, which consists of an ellipsoid and a paraboloid sharing their axes along z-axis and with a common focus O at the origin. The main reflector and subreflector surfaces have been reshaped under the bifocal concept as described in [6]. After developing the iterative shaping procedure, which produces a number of points in the offset profile of the main reflector and subreflector, rotationally symmetric surfaces are defined and represented numerically as follows:

$$Z_M(x,y) = C - A\sqrt{1-\frac{x^2+y^2}{B^2}} + A_0 + A_1(x^2+y^2) + A_2(x^2+y^2)^2 \quad (1)$$

$$Z_S(x,y) = B_0 + B_1(x^2+y^2) + B_2(x^2+y^2)^2 \quad (2)$$

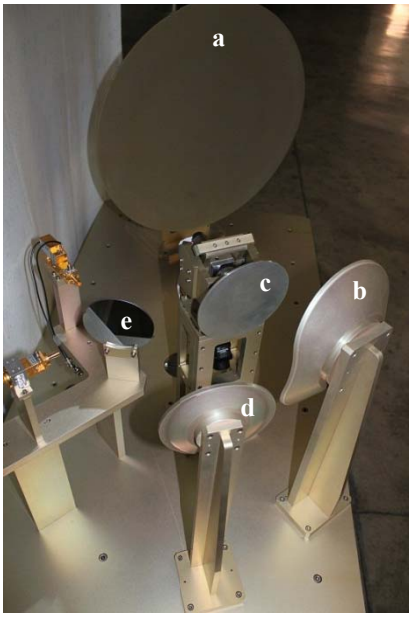

Figure 3. Offset profile of the reflector system

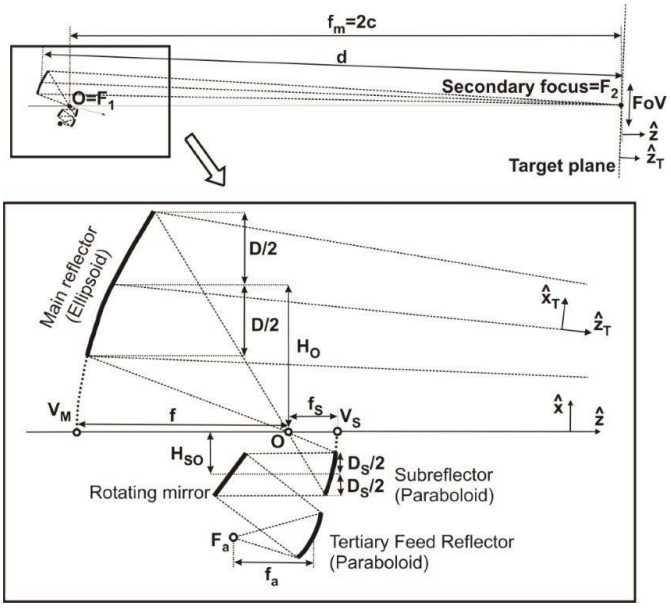

Figure 4. Baseline antenna configuration: offset plane profile view

The first two terms of the main reflector surface equation $Z_M(x)$ describe the original ellipsoid while the last three terms represent the surface modification due to the shaping procedure. Similarly the subreflector surface, which originally

is a second order polynomial corresponding to a paraboloidal one is modified to a fourth order polynomial for representing the shaped surface. The shaped configuration provides a focal ring parallel to the XY plane with radius 30 cm around the target point. An offset section is then selected to avoid blockage problems.

C. *Flat mirror motion for beam scanning*

The mirror surface can be oriented according two axes mechanisms. The mirror is tilted an angle β respect to its ideal unscanned orientation to deviate the beam 25 cm upwards in the offset plane (which is the horizontal one in the prototype picture of Fig. 3). Then, a rapid rotation of the mirror is available about an axis which is coincident with the normal vector of the mirror for its unscanned orientation. The rotation angle is denoted by ϕ and the mirror rotation produces an elliptical trajectory (due to the offset configuration) of the spot in the target plane. The second mechanism is able to tilt the rotation axis an angle γ up and down (perpendicularly to the offset plane) in order to displace the elliptical trajectory vertically, allowing the target plane scanning of the spot and the vertical extension of the scanning area in the target plane, as shown in Fig. 5. Due to the mirror scanning, the subreflector surface must be oversized with more emphasis in its vertical dimension.

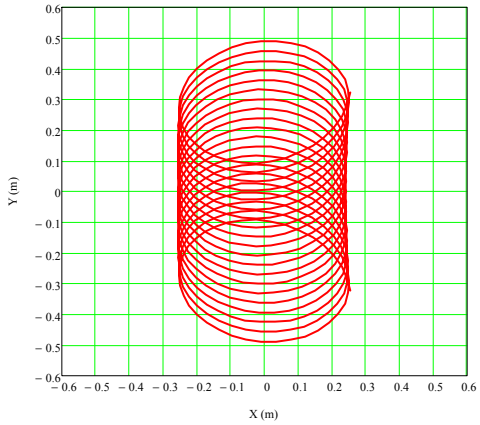

Figure 5. Scanning trajectory of the beam

A center of rotation of the mirror remains in the same location while ϕ and γ mechanisms actuate. A local reference system axis is defined at the mirror for angular reference: the mirror z axis is coincident with the rotation axis for γ=0, the mirror y axis is perpendicular to the offset plane and the local x axis is coincident with the tilting axis for the γ-motion. The x and y components of the normal vector to the mirror are denoted as auxiliary u and v variables describing the mirror motion:

$$u = -\sin\beta\cos\phi \qquad v = -\sin\gamma\cos\beta - \cos\gamma\sin\beta\sin\phi \tag{3}$$

The mapping transformation between the virtual uv-plane and the target plane has been predicted by Geometrical Optics and approximated by simple polynomials in order to simplify the calibration of the system. The polynomial approximation of the mapping transformation is as follows:

$$\begin{aligned} x_t &= a_0 + a_1 u + a_2 u^2 + a_3 v^2 + a_4 u^3 + a_5 u v^2 \\ y_t &= b_1 v + b_2 u v + b_3 u^2 v + b_4 v^3 \end{aligned} \tag{4}$$

Fig. 6 represents the mapping transformation across the target plane when a regular 20x20 lattice in the virtual uv-plane is considered with $-0.1 \le u \le 0.1$ and $-0.2 \le v \le 0.2$. Both the GO ray tracing simulated transformation and the polynomial approximation are represented showing almost perfect agreement.

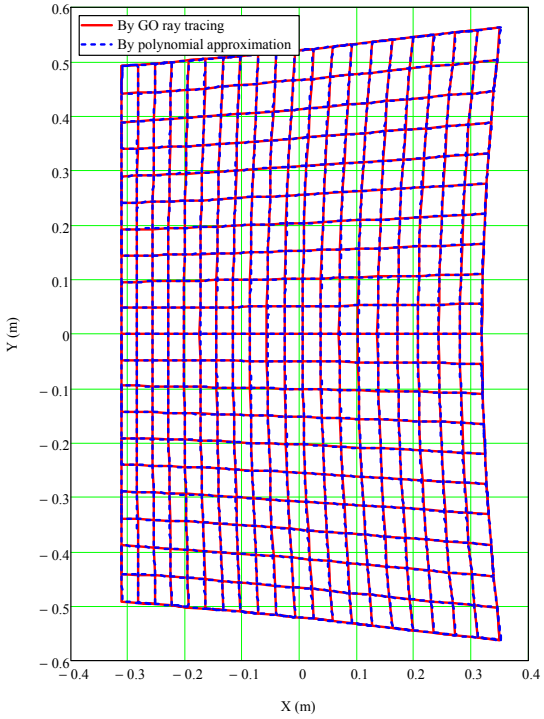

Figure 6. Mapping transformation between mirror motion and target plane. The target plane lattice is represented for a 20x20 lattice in the virtual uv-plane with $-0.1 \le u \le 0.1$ and $-0.2 \le v \le 0.2$

D. *Geometrical Optics simulation of the antenna scanning performance*

For a helical scanning trajectory as described in Fig. 5, a ray tracing procedure has been developed for 720 different mirror orientations along 20 ϕ-turns of the mirror. After tracing up to 127 rays for each mirror orientation, the mean impact point of the bundle of rays on the target plane is an estimation of the spot trajectory represented in Fig. 5. The path length r.m.s. (PLRMS) of the bundle of rays is also accounted as a quality parameter of the scanning because is directly related to the phase aberration of the antenna pattern as described in [6]. The resulting PLRMS of the antenna vs. the radial scan in the target plane is presented in Fig. 7, showing a minimum at 0.3 m corresponding to the radius of the focal ring provided by the bifocal shaping. This behavior allows improving the field of view of the antenna as mentioned in [6].

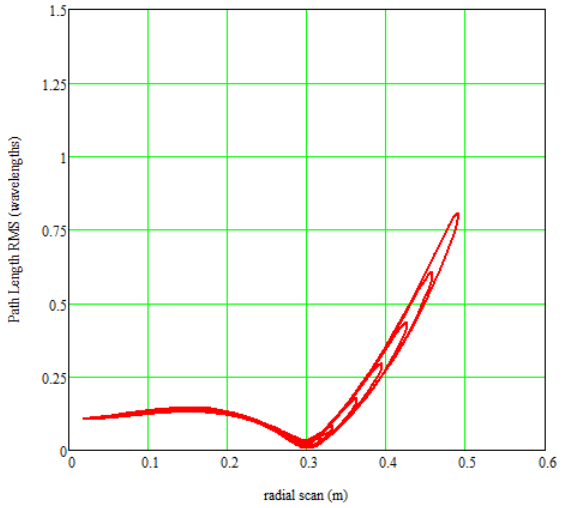

Figure 7. Path length r.m.s. of the antenna by GO simulation

E. *Physical Optics simulation of the antenna scanning performance*

The Physical Optics performance of the antenna has been simulated, based on [7]. Fig. 8 describes the antenna behavior for eight points of the central trajectory (γ=0°) showing the spot beams, their amplitude and beamwidth. Fig. 9 shows a similar result for a displaced trajectory. In all cases the beamwidth of the antenna spot remains in reasonable values.

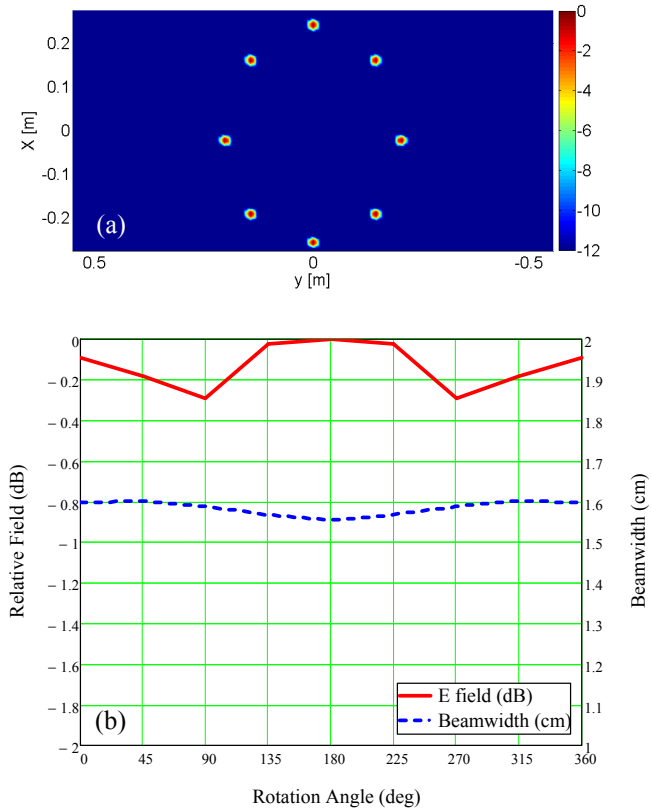

Figure 8. PO simulation for a centered elliptical trajectrory of the spot: (a) scanned beams and (b) Relative E-field and beamwidth

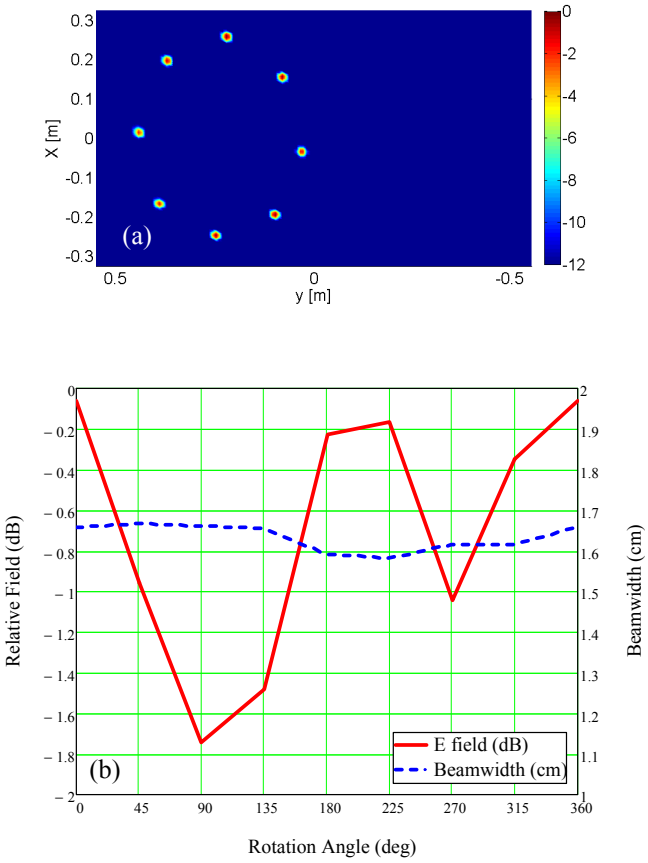

Figure 9. PO simulation for a *y*-displaced elliptical trajectrory of the spot: (a) scanned beams and (b) Relative E-field and beamwidth

IV. CONCLUSION

An imaging radar system at 300 GHz has been developed and constructed. The radar and antenna subsystems have been described, showing images of the prototype. The antenna configuration consists of a confocal reflector system shaped under the bifocal criterion for improving of the field of view. A two axis rotating mirror allows the scanning operation of the imaging radar by implementing an helical trajectory across the target plane. The mapping transformation between the angular motion of the mirror and the beam spot across the target plane has been predicted as well as the antenna performance under GO and PO methods. Now the prototype is being calibrated and tested and preliminary experimental results are expected soon.

ACKNOWLEDGMENT

This work is partially supported by the Spanish National Research and Development Program under project TEC2011-28683-C02-01/02 and Terasense CSD2008-00068 (Consolider-Ingenio 2010).

REFERENCES

[1] P. H. Siegel, "THz technology," *IEEE Trans. Microw. Theory Tech.,* vol. 50, no. 3, pp. 910–928, Mar. 2002.

[2] R. Appleby and H. B. Wallace, "Standoff detection of weapons and contraband in the 100 GHz to 1 THz region," *IEEE Trans. Antennas Propag*., vol. 55, no. 11, pp. 2944–2956, Nov. 2007.

[3] Mencia-Oliva, B.; Grajal, J.; Yeste-Ojeda, O. A.; Rubio-Cidre, G.; Badolato, A.; , "Low-Cost CW-LFM Radar Sensor at 100 GHz," *to apear in Microwave Theory and Techniques, IEEE Transactions on* , vol. 61, no. 2 , 2013.

[4] Mencia-Oliva, B.; Grajal, J.; Yeste-Ojeda, O.A.; Rubio-Cidre, G.; Badolato, A., "Multiple purpose hardware for sensors at 100 GHz," *Radar Conference, 2012 IET International* , vol., no., pp. , 22-25 October 2012

[5] N. Llombart, K. B. Cooper, R. J. Dengler, T. Bryllert, and P. H. Siegel, "Confocal ellipsoidal reflector system for a mechanically scanned active terahertz imager," *IEEE Transactions on Antennas and Propagation*, vol 58, no. 6 99, pp. 1834-1841, June 2010.

[6] A.G.Pino, N.LLombart, B.Gonzalez-Valdes and O. Rubiños; "A Bifocal Ellipsoidal Gregorian Reflector System for THz Imaging Applications," *IEEE Transactions on Antennas and Propagation*, vol. 60, no. 9, pp. 4119–4129, Sep. 2012.

[7] J.A.Martínez, A. G. Pino, I.Vega, M.Arias, O.Rubiños, "ICARA: Induced current analyis of reflector antennas", *IEEE Antennas and Propagation Magazine*, Vol.47, no.2 pp.92-100. April 2005.